

Electroencephalographic Response of Brain Stimulation by Shock Waves From Laser Generated Carbon Nanotube Transducer

JooHo Lee¹, John W. Larocco², and Dong-Guk Paeng³, *Member, IEEE*

Abstract—Neuromodulation is used to treat neurological disorders. Focused ultrasound can deliver acoustic energy to local regions of the brain, including deep brain structures. In addition, it is possible to induce the activation or inhibition of nerves through parameter adjustments of focused ultrasound. Laser-generated focused ultrasound (LGFUS) has demonstrated a potential use in precise therapeutic ultrasound applications owing to the ability to produce high-pressure, broadband frequency of shock waves with a tight focal spot, resulting in confined acoustic exposure of a small area. However, there have been few studies of neurostimulation using shock waves with pulse durations of several nanoseconds. The purpose of this study is to investigate the possibility of neurostimulation by shock waves generated from a focused Carbon Nanotube (fCNT) transducer. We measured electroencephalographic (EEG) signals in three rat brains before and after shock wave stimulation and compared them in the time and frequency domains. In the time domain, the number of peaks of EEG signals was measured significantly higher after shock wave stimulation than before stimulation in all three rats. The three rats showed differences in three frequency bands: theta(4-7 Hz), alpha(8-12), and 1–30 Hz, before and after shock wave stimulation ($p < 0.001$). These differences in EEG signals after shock wave stimulation of three rats were confirmed mainly because of shock waves. The stimulation of a rat brain was feasible using shock waves generated by the fCNT transducer. This study provides a basis for the applications of shock waves to brain stimulation for precise targeting.

Index Terms—Focused carbon nanotube transducer, electroencephalographic, shock wave, brain stimulation, laser-generated focused ultrasound.

Manuscript received 17 March 2022; revised 10 October 2022; accepted 1 November 2022. Date of publication 24 November 2022; date of current version 31 January 2023. This work was supported in part by the Focused Ultrasound Foundation and in part by the NRF Grant through the Korea Government under Grant MSIT 2018R1A2B2007997 and Grant 2022R1A5A1022977. (Corresponding author: Dong-Guk Paeng.)

JooHo Lee is with the Department of Ocean System Engineering, Jeju National University, Jeju 63243, South Korea (e-mail: ljooHo@jejunu.ac.kr).

John W. Larocco is with the Ronin Institute, Montclair, NJ 07043 USA (e-mail: dr.john.larocco@protonmail.com).

Dong-Guk Paeng is with the Department of Ocean System Engineering, Jeju National University, Jeju 63243, South Korea, and also with the Department of Radiology and Medical Imaging, University of Virginia, Charlottesville, VA 22904 USA (e-mail: paeng@jejunu.ac.kr).

Digital Object Identifier 10.1109/TNSRE.2022.3224897

I. INTRODUCTION

NEUROMODULATION has been used to treat neurological disorders. For several decades, deep brain stimulation (DBS) [1] and vagus nerve stimulation (VNS) [2] have been used to treat neurological disorders. To avoid the side effects of these invasive treatments, noninvasive brain stimulation methods, such as transcranial magnetic stimulation (TMS) [3], [4] and transcranial direct-current stimulation (tDCS) [5], [6], have been used to treat neurological disorders and to control the function of cortical regions of the brain [7], [8]. In electromagnetic stimulation techniques, the size of the stimulation area is relatively large compared to the size of the target, and the ability to reach deep brain areas is limited [8], [9].

Focused ultrasound can deliver acoustic energy to local regions of the brain, including deep brain structures. Low-intensity transcranial focused ultrasound (tFUS) has shown that acoustic pressure waves do not cause temperature elevation but stimulate brain functions without side effects such as thermal ablation [10], [12], [13], [14], [15], [16]. tFUS can provide better spatial resolution at a deeper target area than other noninvasive technologies. The energy of acoustic pulse waves is transmitted through the skull, and the target position can be adjusted by the phase correction of multi-element array systems. In addition, it is possible to induce the activation or inhibition of nerves by adjusting the parameters of focused ultrasound (FUS) [13], [14].

Continuous or long-pulse ultrasound waves have been used for neuromodulation [17], [18]. Ultrasound neuromodulation has been studied with parameters such as ultrasound fundamental frequency (f_0) [19], ultrasound duration (UD) [14], duty cycle (DC) [20], [21], and pulse repetition frequency (PRF) [21]. Since it is necessary to evaluate the characteristics of ultrasound for neuromodulation, research has been conducted to optimize the intensity/energy, UD, and PRF for successful neuromodulation. Kim et al. observed that a motor response was elicited at minimum threshold acoustic intensities in the limited ultrasound parameters ($f_0 = 350$ kHz, UD = 300 ms, etc.) [13]. Another study confirmed the success rate of neurostimulation according to the characteristics of ultrasound, such as frequency band, acoustic intensity, and UD [14]. Many studies have been conducted by controlling the intensity, PRF and pulse duration to determine the key parameters of ultrasound stimulation. [13], [14]. Neurostimulation studies

using pulsed ultrasound show a low success rate below specific threshold values of the parameters of acoustic intensity and duration. When intensity is less than 4.2 W/cm^2 , the success rate of ultrasound stimulation is less than 66%. When sonication duration is less than 80 ms, the success rate is less than 77% [13], [14].

Shock waves have been used in brain applications. They have a wide frequency band and a short rising time of less than a few nanoseconds. Shock waves for lithotripsy have been used to verify the blood–brain barrier opening [22]. Furthermore, the stability and efficacy of producing target lesions in the brain using histotripsy have been demonstrated [23]. Laser-generated focused ultrasound (LGFUS) transducers have demonstrated a potential use in precise therapeutic ultrasound applications, owing to their ability to produce high-pressure, high-frequency shock waves with a tight focal spot, resulting in confined acoustic exposure at a small area [24]. LGFUS transducers can be used for high-precision therapies, including lithotripsy [25], cell manipulation [26], remotely controlled drug delivery [27], and efficient sonothrombolysis [25]. However, few studies have been conducted on neurostimulation by shock waves generated by LGFUS.

Although shock waves generated by focused carbon nano tube (fCNT) transducers have higher acoustic pressure than conventional ultrasound, they involve short pulses of several nanoseconds, which have not yet been explored for neurostimulation. The purpose of this study is to investigate the possibility of neurostimulation by shock waves generated from an fCNT transducer. We measured electroencephalographic (EEG) signals in rat brains before shock wave stimulation and compared them to EEG signals after stimulation. This is a pilot study to confirm whether shock waves with a broader band at a low PRF can affect the EEG signals from three rat brains.

II. METHOD

A. Animal Preparation

This neurostimulation experiment was approved by the Jeju National University Institutional Animal Care and Use Committee (IACUC). All procedures and rat handling were performed following the ethical guidelines for animal studies. Rats were anesthetized intramuscularly during all procedures with a mixture of Zoletil 25 mg/kg (Virbac Laboratories, France) and Rumpun 4.6 mg/kg (Bayer, Leverkusen, Germany) and were monitored throughout the experiment. No pain or suffering was evident as a result of the procedure. A total of 3 male Sprague-Dawley rats (450g weight, Orient Bio Inc., Seongnam, Korea) were used for this study. The hair on their heads was removed using a shaving razor and hair removal cream. The rats used in the experiment were euthanized by injecting CO_2 into an airtight container. The fCNT transducer was fabricated by the method used in the studies of Kim et al. [28].

B. EEG Measurement Setup

EEG electrodes are positioned in consistent places based on the anatomy and size of the subject's head. Among the most popular layout conventions is the 10–20 International

System [29]. Other electrode layouts exist for humans, primates, and other laboratory animals, including rats [30]. The acquisition system utilized an OpenBCI Ganglion board, which permitted the recording of up to four EEG channels at 200 samples per second. The OpenBCI EEG system has previously been used for brain-computer interfaces (BCIs) and drowsiness detection [31], [32]. In this study, the three electrodes were placed at T6, T5 and Reference region [33] of the rat's head, and a ground electrode was on the ear. Data were acquired over Bluetooth using the OpenBCI GUI on a Windows 10 laptop [34]. Fig. 1(a) shows the EEG measurement setup for comparing signals from before and after the shock wave stimulation. To obtain reference data before stimulation, EEG signal response was measured for 10 min after anesthesia. Each rat was sonicated for 10 min. Stimulation was accomplished by LGFUS from an fCNT transducer driven by a laser pulse source. The fCNT transducer position of shock wave stimulation was 3 mm left of the bregma in the rat brain. The brain stimulation area of LGFUS was the somatosensory cortex, which is positioned at 3 mm from the skull surface. After Stimulation, EEG signals from all three rats were recorded for 20 min. Each subject provided two sessions of EEG: pre-stimulation and post-stimulation. The range of noise was used to fit a 30th order Blackman-window bandpass filter between 1–45 Hz for offline processing. During recording, a 1–50 Hz bandpass filter was used to remove overhead line noise. The EEG channel with the lowest noise was calculated by finding the channel with minimal variance after bandpass filtering and removing the means. Then, the power spectrum of the EEG was calculated using a one-second sliding window, with a 50% overlap with the prior window. Each one-second period was referred to as a single trial or epoch. Welch's method was used to estimate the power spectrum. Prior to experimentation, two-minute EEG signals from an unsedated rat were acquired [35]. The locations of the EEG measurements are shown in Fig. 1(a), and a flow chart for measuring the EEG signal is shown in Fig. 1(b). EEG signals were measured at three points. The red circles indicate the EEG measurement positions and the green circle indicates the ultrasound stimulus location. Three electrodes were subjected to EEG. By comparing the data received from each electrode, EEG channel with the most significant difference before and after shock wave stimulation was selected and analyzed.

EEG signals from pre- and post-stimulation were compared in the time domain. To confirm EEG signal changes in the rat brain from shock wave stimulation, the number of peaks of the EEG signal was counted before and after shock wave stimulation. To count the number of peaks, the standard deviation ($6.7 \mu\text{V}$) of the reference signal with the highest voltage was selected as the threshold. The peaks exceeding the threshold were counted, and the number of peaks before and after stimulation was compared. Among the EEG bands, the theta(4–7 Hz) and alpha(8–12 Hz) bands, which are related to resting, breathing, and awareness training tasks [23], [36], [37], and a frequency band of 1–30 Hz, including most of the frequency band, were selected. In the frequency domain, power spectral density (PSD) and root mean square (RMS) values in each alpha, theta, and 1–30 Hz

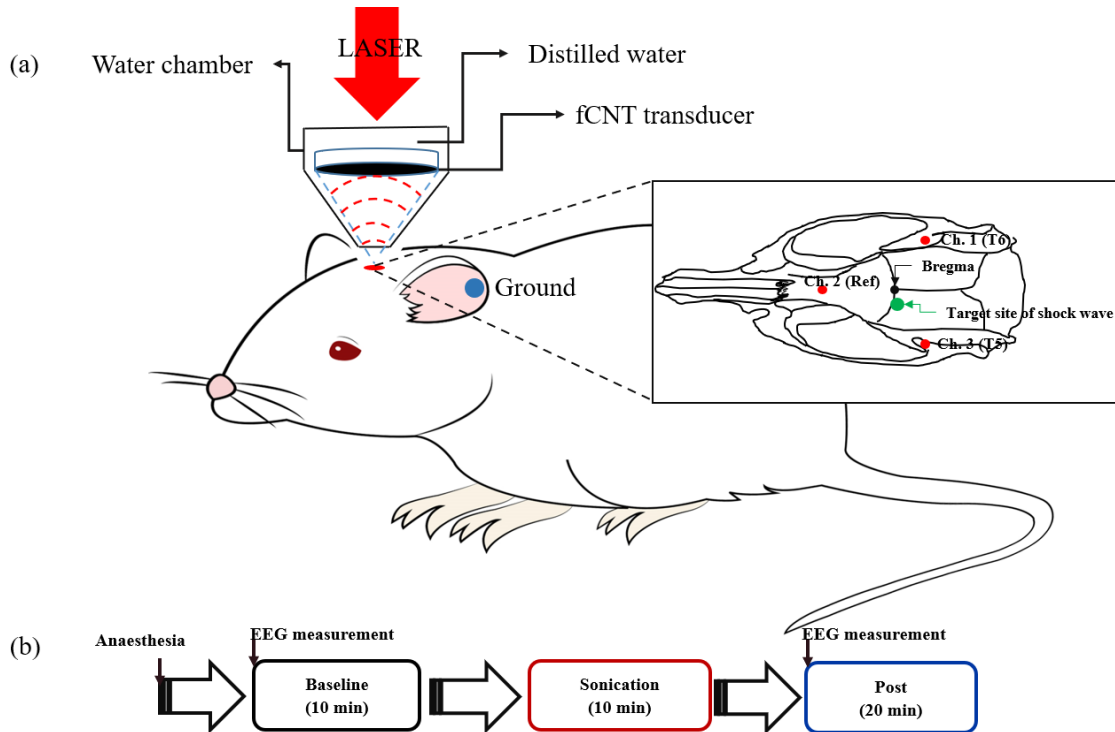


Fig. 1. (a) Experimental setup for measuring Electroencephalographic (EEG) signals upon brain stimulation of shock waves generated by focused Carbon Nanotube (fCNT) transducers. (b) Flowchart of the EEG acquisition and shock wave stimulation. The Red circles is EEG measurement sites, green circle is target position of shock waves.

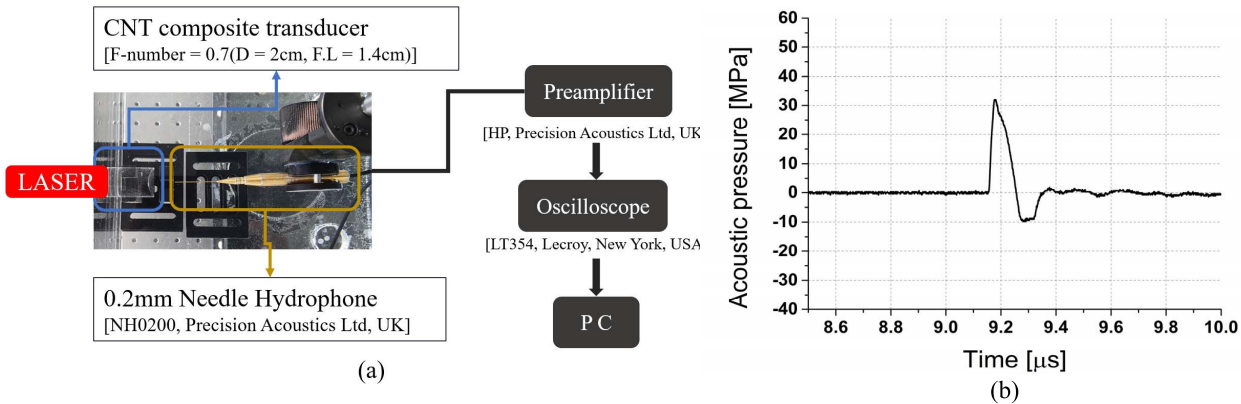


Fig. 2. (a) Measurement set up for shock waves from laser-generated by fCNT transducer (Laser energy : 350 mJ, PRF : 5 Hz, Wavelength : 532 nm). (b) Shock wave when laser energy is 350 mJ.

frequency band before and after shock wave stimulation were compared.

C. Shock Wave Measurement Setup

The experimental setup is shown in Fig. 2(a). When the laser was applied to the fCNT transducer ($F\# = 0.7$, focal length = 1.4 cm) which was immersed in water, the fCNT layer produced a LGFUS. A pulse laser system (Tribeam, Jeisys, Medical Inc., Seoul, Korea) with a wavelength of 532 nm and energy of 350 mJ was used to generate a shock pulse with a PRF of 5 Hz. The shock wave generated by the CNT-PDMS composite transducer has a beam width of 2.5 mm in the axial direction and 0.70 mm in the lateral direction [38]. A needle hydrophone (NH0200, Precision Acoustics Ltd, UK) was used to measure the shock pulse. The hydrophone was

used with a 20 dB preamplifier (HP, Precision Acoustics Ltd, UK) powered by a DC coupler (Precision Acoustics Ltd, UK). The signal was monitored using an oscilloscope (LT354, Lecroy, New York, NY, USA). The peak positive and negative pressures of LGFUS are 30 MPa and -8 MPa, respectively. The center frequency is 4 MHz and -6 dB bandwidth is 7 MHz.

III. RESULTS

Brain responses before and after stimulation with shock waves generated by the fCNT transducers were confirmed by EEG signal changes. For the results, EEG signals from three rats before and after stimulation were compared in the frequency and time domains. In the frequency domain, signal responses in theta (4~8 Hz), alpha (8~12 Hz), and 1~30 Hz

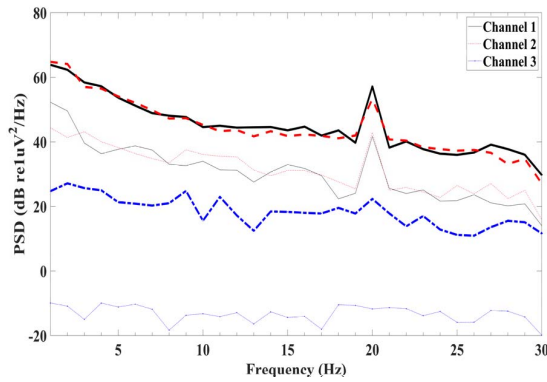


Fig. 3. PSD comparison of 3 channels before and after shock wave stimulation of EEG signals measured at Rat 1. The thick line is the PSD after stimulation, and the thin line is the PSD before stimulation.

bands were compared. In the time domain, the amplitudes and numbers of peaks were compared.

The EEG signals measured in three channels were compared in the frequency domain. Fig. 3 shows the differences in EEG signals before and after shock wave stimulation in the 1–30 Hz band in Rat 1. The differences between the EEG signals measured in the three channels before and after stimulation are clearly shown. In channels 1 and 2, the PSD of 1–30 Hz band was similarly measured. However, the PSD measured before and after stimulation in channel 3 was the lowest, but the difference was the largest among the three channels. Table I shows the differences in PSD before and after stimulation for all the rats in three bands, including the 1–30 Hz band, of 3 channels. Except for channel 1 (theta and alpha bands) and channel 2 (alpha band) of Rat 2, the PSD after shock wave stimulation was higher than before stimulation. Areas showing a clear difference of 15 dB or more are shaded. In all frequency bands for all rats, the shaded areas show the largest differences in channel 3. Therefore, the subsequent results were compared by selecting only the results measured in channel 3.

A. Comparison in the Frequency Domain

Fig. 4 shows the results of the EEG signal responses of three rats in the 1–30 Hz band before and after shock wave stimulation. The EEG signal responses after stimulation were higher than those before stimulation in the entire range of 1–30 Hz. The differences between signal responses before and after stimulation were 31.6 ± 4.2 , 14.7 ± 11.0 , and 14.8 ± 4.4 dB for three rats. The PSD values of EEG signals measured before and after stimulation were distributed below and above 0 dB, respectively. Among the three rats, Rat 1 had the largest difference in PSD values before and after stimulation, while Rat 3 had the smallest difference.

Theta and alpha bands were extracted from the measured EEG signal responses shown in Fig. 5, and the effects before and after shock wave stimulation were compared. Fig. 5(a) compares EEG signal responses in the theta band. The differences in EEG signal responses before and after stimulation for Rats 1, 2, and 3 were 32.6 ± 1.6 dB, 22.2 ± 1.5 dB, and 19.6 ± 4.7 dB (ref $1 \mu V^2/Hz$), respectively. In Rats 2 and 3,

TABLE I
DIFFERENCE IN POWER BEFORE AND AFTER THE SHOCK WAVE STIMULATION OF 3 RATS MEASURED IN 3 CHANNELS. AREAS WITH A DIFFERENCE OF 15 dB OR MORE BEFORE AND AFTER STIMULATION ARE SHADED

Difference power before and after shock wave stimulation [(Integrated PSD _{AFTER} - Integrated PSD _{BEFORE})/Hz]			
Rat	CH.1	CH.2	CH.3
Rat 1	Theta band	15.1	34
	Alpha band	13.5	34.8
	1-30 Hz band	14.6	31.7
Rat 2	Theta band	-2.2	22.5
	Alpha band	-3.7	20.8
	1-30 Hz band	3	17.6
Rat 3	Theta band	5.6	19.5
	Alpha band	6.3	15.9
	1-30 Hz band	4.7	14.8

the average difference in the theta bands before and after stimulation was lower than that of the alpha band. Fig. 5(b) shows a comparison between the PSD before and after stimulation in the alpha band. For Rat 1, the difference in PSD between before and after stimulation was 34.7 ± 4.9 dB (ref $1 \mu V^2/Hz$). Rats 2 and 3 had similar differences, 20.7 ± 2.7 dB and 15.9 ± 2.6 dB (ref $1 \mu V^2/Hz$), respectively. In the other rat, the average difference in the overall theta band was similar to the difference in the alpha band. In the channel 3 of Table I, the dB differences before and after stimulation of the three rats at all frequency intervals were positive. In all frequency bands, there was a difference in magnitude in the order of Rats 1, 2, and 3. This result indicates that the magnitude of the signal increased after shock wave stimulation.

The power of the EEG signals before and after shock wave stimulation in each rat was calculated and compared. Fig. 8 shows the results of calculated power of the EEG signal responses in the theta (Fig. 6(a)) and alpha (Fig. 6(b)) band sections. The calculated power before and after stimulation is shown separately for each rat. It can be seen that Rat 1 has the highest difference in both theta (4–7 Hz) and alpha (8–12 Hz) bands, and Rat 2 and 3 also showed significant differences. The power of the theta bands of Rats 2 and 3 was greater than that of the alpha band.

B. Comparison in the Time Domain

The raw EEG signal data measured before and after stimulation with shock waves are shown in Fig. 7. Fig. 7(a), 7(b), and 7(c) show the time domain data for Rats 1, 2, and 3, respectively, and demonstrate obvious differences in amplitudes before and after stimulation. In all three

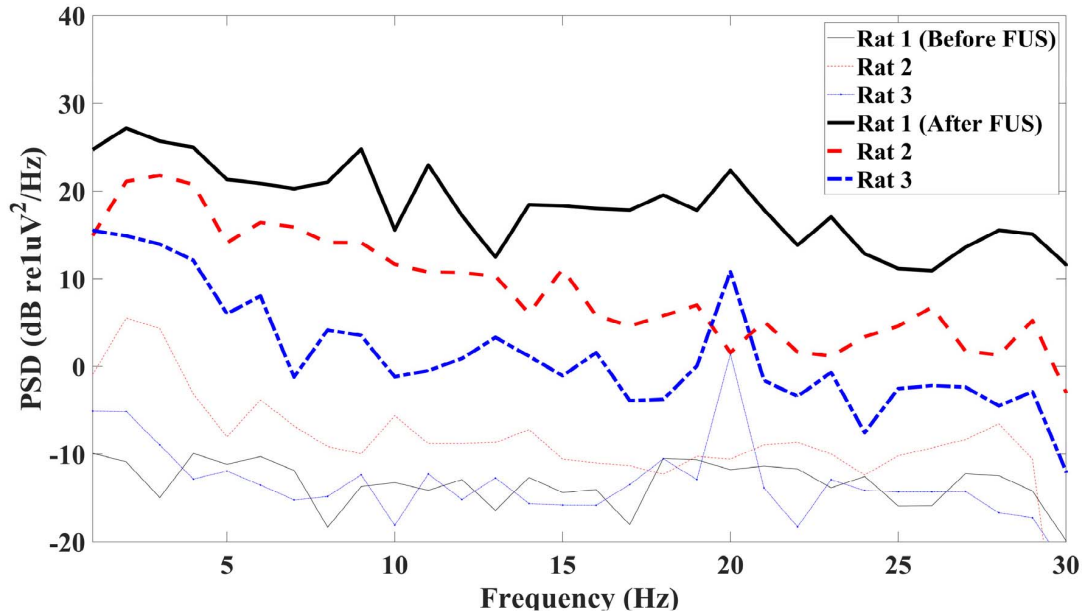


Fig. 4. PSD of the EEG signal responses of 3 rats in 1-30 Hz band before and after shock wave stimulation ($p < 0.001$). The dotted line on the vertical axis indicates the PSD section in each theta band and the alpha band. The thick line is the PSD after stimulation, and the thin line is the PSD before stimulation.

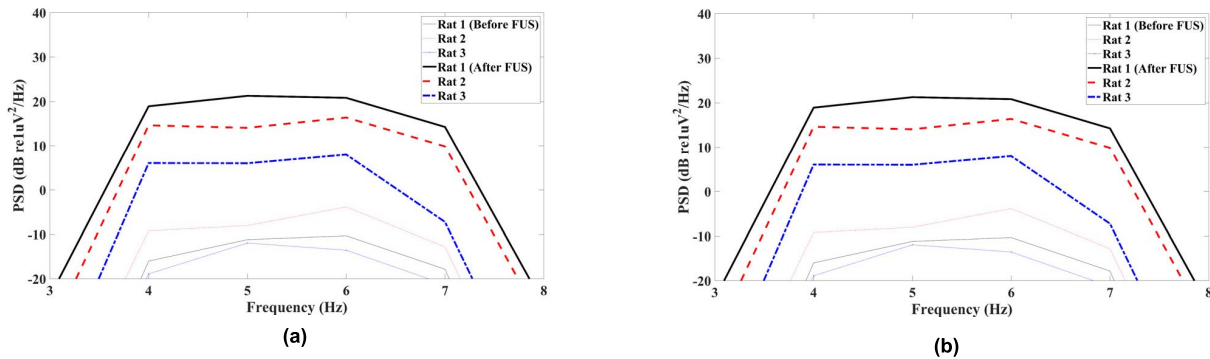


Fig. 5. PSD of the EEG signal responses of 3 rats before and after shock wave stimulation. (a) Theta(4-7 Hz) band. (b) Alpha (8-12 Hz) band. ($p < 0.001$). The thick line is the PSD after stimulation, and the thin line is the PSD before stimulation.

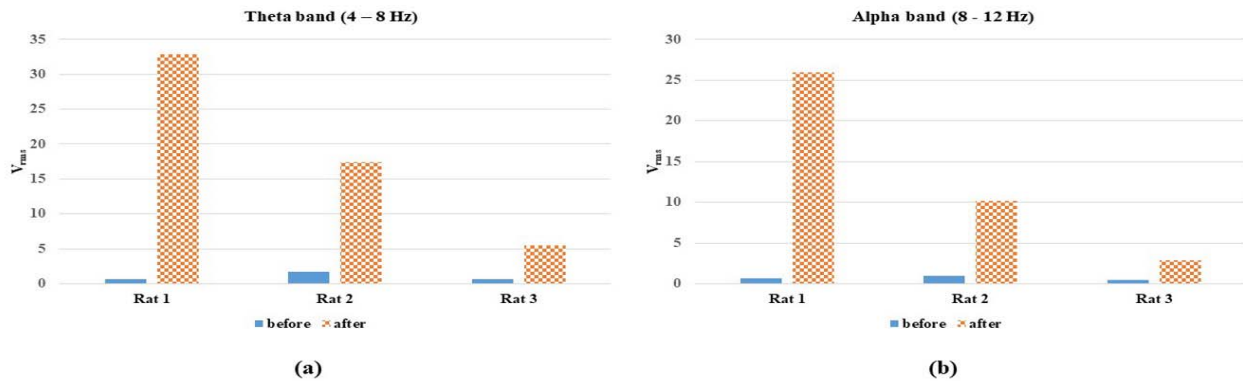


Fig. 6. Comparison of the power (RMS) of EEG signals before and after shock wave stimulation. (a) Power at the theta (4-7 Hz) band. (b) Power at the alpha (8-12 Hz) band.

rats, it was confirmed that the amplitudes of EEG signals after shock wave stimulation were higher than before stimulation. To measure the number of peaks under the influence of stimulation, the amplitude peaks with values higher than the standard deviation ($\pm 6.7 \mu\text{V}$) were counted, as shown in Table II. It was confirmed that there were more peaks after

shock wave stimulation than before stimulation in all rats, although the differences in the number of peaks before and after shock wave stimulation varied among the rats.

Fig. 8 shows the change in the average number of peaks before and after shock wave stimulation by dividing the data according to time. The average number of peaks before

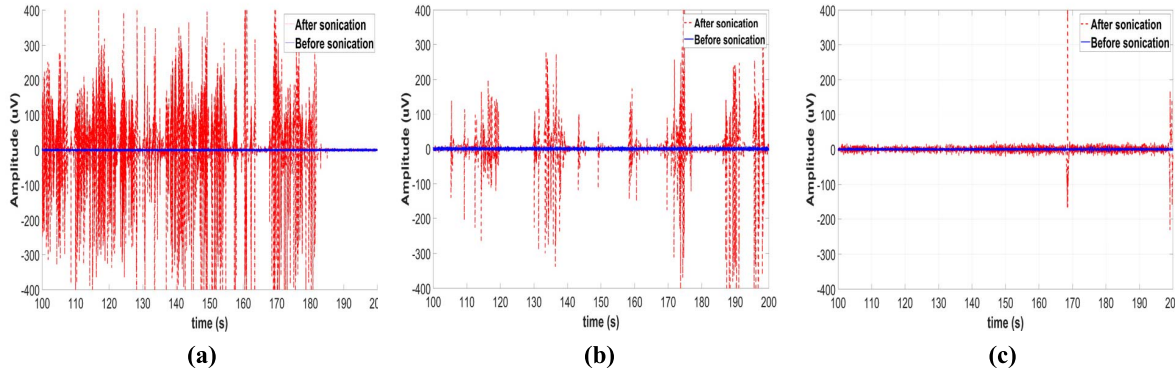


Fig. 7. Comparison of amplitude change of EEG raw signal before and after shock wave stimulation in time domain. Bold blue lines and red dotted lines are the signals before and after shock wave stimulation, respectively.

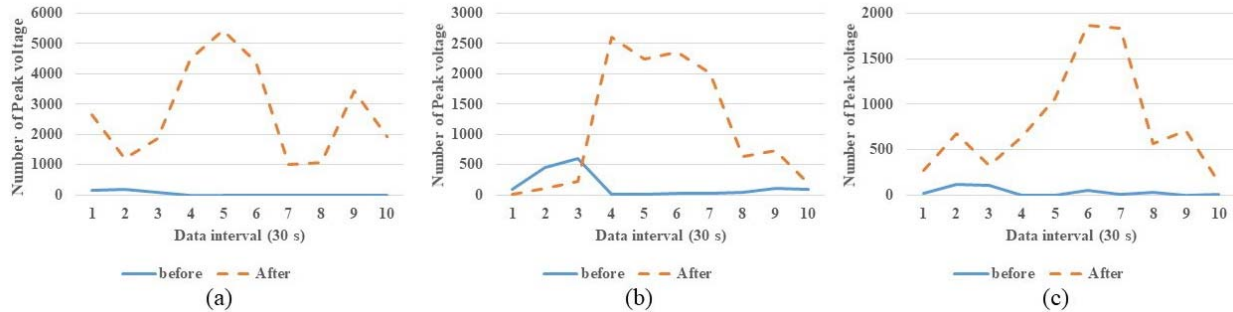


Fig. 8. Total number of peaks at 30 sec intervals before and after shock wave stimulation of each rat. (a) number of peaks before and after stimulation for rat 1. (b) Rat 2. (c) Rat 3. The x-axis shows 5 minutes data divided into 10 sections with 30 second intervals, and the y-axis is the average number of peaks for 30 seconds.

TABLE II

DATA ON THE NUMBER OF PEAKS IN THE 5 MINUTES BEFORE AND AFTER SHOCK WAVE STIMULATION FOR EACH RAT (OVER $\pm 6.6 \mu\text{V}$)

Number of peaks (over $\pm 6.6 \mu\text{V}$)	Before (Count)	After (Count)
Rat 1	424	27444
Rat 2	1493	11130
Rat 3	329	8077

and after each shock wave stimulation was calculated by dividing the five minutes of data measured for each rat into 30-second intervals. For each rat, the number of peaks after stimulation was higher than before stimulation. For all rats, it was confirmed that the difference in the average numbers of peaks in the middle data interval (interval 4 to 7) before and after stimulation was larger than in other sections. In case of Rat 2, the average number of peaks before stimulation was higher than after stimulation in the data interval 1 to 3. Based on the results for data interval 1 to 3 for Rat 2, it was confirmed that the difference in the average number of peaks before and after stimulation for the entire time was smaller for Rat 2 than for other rats.

IV. DISCUSSION

This study is a preliminary study to confirm the feasibility of brain stimulation with shock waves generated from fCNT

transducers. We measured and compared EEG signals from the rat brains before and after stimulation by shock waves generated by an fCNT transducer. In the time domain, the number of peaks of EEG signals after shock wave stimulation of all three rats was significantly higher than before stimulation. Three rats showed differences in PSD and RMS values before and after shock wave stimulation ($p < 0.001$) in three frequency bands: alpha, theta, and 1–30 Hz. These differences in EEG signals before and after shock wave stimulation of the three rats are mainly due to the effect of shock waves. However, the number of rats used was limited to three, and it was insufficient to study the parameters that stimulate specific brain regions to the extent that behavioral observations are possible. Because histological analysis was not performed, it was not possible to accurately reveal the tissue damage. Despite these limitations, the feasibility of brain stimulation was confirmed by the characteristics of the shock wave generated by the fCNT transducer, and to the best of our knowledge, this is the first study to be attempted.

In contrast to conventional ultrasonic transducers, fCNT transducer is easier to fabricate. It produces a very short pulse wave of less than 80 ns. In our system, it has a PRF of 5 Hz, but the PRF can be increased depending on the system. The intensity of ultrasound used for conventional neurostimulation is about 4.9 to 5.6 W/cm^2 [13] and the pulse duration is 20 ms to 320 ms [14], using various parameters. In a previous study, the intensity range without tissue damage was 2.5–2.8 W/cm^2 (I_{spta}) [14]. The intensity of the

shock wave used in this study was 8 mW/cm^2 ($I_{\text{spta}})(I_{\text{sptp}} = 68 \text{ kW/cm}^2$, $I_{\text{sppa}} = 10.7 \text{ kW/cm}^2$), which is smaller than that used in a previous study. In addition, there was no histological damage at the sound pressure of the shock wave without cavitation (-9.79 MPa) [22], [39]. The shock wave generated by the fCNT transducer generates a much shorter pulse than the pulse generated by the conventional transducer. fCNT transducers are easy to manufacture by changing the shape of the transducer, and ultrasound waves can be easily generated by irradiating laser energy alone. fCNT transducers can also be applied to various preclinical and clinical studies because they can be easily designed and fabricated as wearable transducers [40].

Tissue heating caused by shock waves is associated with boiling histotripsy. Boiling histotripsy has a negative pressure of $10\text{--}20 \text{ MPa}$ and a positive pressure of 70 MPa or more [41]. In addition, the duty cycle of the shock wave is very low, and the peak positive pressure of the shock wave used in this study is 30 MPa and the negative pressure is -9 MPa . Therefore, it has characteristics suitable for in vivo applications that prevent ultrasound heating of biological tissue. Tissue damage can occur because of the high sound pressure of the shock wave generated from the fCNT transducer, but the degree of damage varies depending on the number of cycle pulses [42], level of sound pressure, and the number of sonication times [22], [42]. The physical damage to tissues by ultrasound is mostly caused by cavitation. For shock-scattering histotripsy, shock waves of 3–10 cycle pulses were used. Positive pressure ($>50 \text{ MPa}$) and negative pressure (-15 to 25 MPa) [42] at much higher levels than the acoustic pressure used in this study were used. Autopsy of the rat brains after stimulation with LGFUS confirmed that there was no apparent damage. This study confirmed the feasibility of brain stimulation through shock waves which are different from conventional ultrasound. When the intensity of the shock wave generated from the CNT composite is compared with other similar studies as a quantitative value, it can be sufficiently predicted that there will be no brain tissue damage. Histological damage can be confirmed, but the other side effects have not yet been studied. There is a possibility that other side effects by a different mechanism may occur even if there is no tissue damage. As in the previous study [43], it is necessary to evaluate the effects by comparing the results of the shock wave stimulation to the auditory cortex and the listening to the sound. A literature review by Blackmore et al. [44] primarily covered brain stimulation mechanisms from the traditional piezoelectric transducers, including minor auditory effects. Therefore, it is necessary to evaluate the intensity of the shock wave by checking the tissue damage through histological analysis. In future experiments, the degree of damage will be derived through quantitative evaluation while controlling the parameters of the shock wave.

EEG signals before and after shock wave stimulation were measured in three channels for all rats. The reason of greater difference in EEG signals in channel 3 before and after shock wave stimulation may be due to the stimulation position of primary somatosensory cortex. Local stimulation to this

primary somatosensory cortex propagates to the contralateral body, which may have smaller response of EEG signals in channel 1. However, this study was designed as a preliminary trial to measure the EEG response by shock wave stimulation in rat brain using an fCNT transducer without the precision targeting nor systematic analysis with histology. As a future study, the response to each EEG channel needs to be confirmed and analyzed by precision target by shock wave from an fCNT transducer.

The EEG signals to analyze the results were measured before and after shock wave stimulation. Simultaneous measurement could not be performed because during shock wave stimulation the EEG signal was affected by the contact between the fCNT transducer and the EEG measuring device. The measurement setup has a limitation in that it is impossible to check for EEG signals changes in real time during shock wave stimulation. However, when the EEG signals of the three rats were analyzed before shock wave stimulation, they showed similar tendencies in the time and frequency domains (Fig. 7 and Fig. 8). When the EEG signals were measured immediately after shock wave stimulation, it was confirmed that the corresponding EEG values were significantly higher (Fig. 7 and Fig. 8, $p < 0.001$).

The results based on the standard deviation of the EEG signals among the three rats before shock wave stimulation in the raw data have the advantage of directly confirming EEG changes due to shock wave stimulation. In Rats 1, 2, and 3, the differences in the number of peaks before and after shock wave stimulation were calculated to be approximately 41, 1.6, and 14.9, respectively. Rat 2 had the highest number of EEG signal peaks before shock wave stimulation and the lowest number after shock wave stimulation. Although each rat showed a difference in the number of EEG peaks before and after shock wave stimulation, the degree of difference in the number of peaks among the rats varied. This is expected from the individual differences in each rat. Further studies are needed to elucidate the cause of this variation. In this experiment, the number of rats used as a preliminary experiment to confirm the brain stimulation effect of shock waves generated from fCNT transducers was insufficient to derive statistical significance. However, the results of the stimulation of the brains of three rats confirmed that changes in EEG signals occur after shock wave stimulation. In future experiments, the experimental setup should be changed to verify real-time changes to ultrasonic stimulation and to confirm the effect of the fCNT-generated shock wave characteristics. The brain stimulation effect of the shock wave can be confirmed by increasing the number of experimental animals to obtain statistical results.

V. CONCLUSION

We stimulated rat brains with shock waves generated by an fCNT transducer and confirmed changes in the theta, alpha and 1–30 Hz bands of the EEG signals before and after shock wave stimulation. This method can be used to stimulate only a very small part of the target, and it will be provided as a means for precise verification of brain function by measuring

the brain stimulation mapping for the location and depth of the brain using the high spatial resolution of the shock wave.

REFERENCES

- [1] K. Ashkan, P. Rogers, H. Bergman, and I. Ughratdar, "Insights into the mechanisms of deep brain stimulation," *Nature Rev. Neurology*, vol. 13, no. 9, pp. 548–554, 2017.
- [2] W. H. Theodore and R. Fisher, "Brain stimulation for epilepsy," *Operative Neuromodulation*, vol. 3, pp. 261–272, Feb. 2007.
- [3] M. Kobayashi and A. Pascual-Leone, "Transcranial magnetic stimulation in neurology," *Lancet Neurol.*, vol. 2, no. 3, pp. 145–156, Mar. 2003.
- [4] A. T. Barker, R. Jalinous, and I. L. Freeston, "Non-invasive magnetic stimulation of human motor cortex," *Lancet*, vol. 325, no. 8437, pp. 1106–1107, 1985.
- [5] M. A. Nitsche and W. Paulus, "Excitability changes induced in the human motor cortex by weak transcranial direct current stimulation," *J. Physiol.*, vol. 527, no. 3, pp. 633–639, Sep. 2000.
- [6] J. C. Horvath, J. D. Forte, and O. Carter, "Evidence that transcranial direct current stimulation (tDCS) generates little-to-no reliable neurophysiologic effect beyond MEP amplitude modulation in healthy human subjects: A systematic review," *Neuropsychologia*, vol. 66, pp. 213–236, Jan. 2015.
- [7] M. S. George and G. Aston-Jones, "Noninvasive techniques for probing neurocircuitry and treating illness: Vagus nerve stimulation (VNS), transcranial magnetic stimulation (TMS) and transcranial direct current stimulation (tDCS)," *Neuropsychopharmacology*, vol. 35, no. 1, pp. 301–16, 2010.
- [8] F. Fregni and A. Pascual-Leone, "Technology insight: Noninvasive brain stimulation in neurology—Perspectives on the therapeutic potential of rTMS and tDCS," *Nature Clin. Pract. Neurol.*, vol. 3, no. 7, pp. 383–393, Jul. 2007.
- [9] K. K. Loo and P. B. Mitchell, "A review of the efficacy of transcranial magnetic stimulation (TMS) treatment for depression, and current and future strategies to optimize efficacy," *J Affect Disord.*, vol. 88, no. 3, pp. 255–267, 2005.
- [10] P. C. Rinaldi, J. P. Jones, F. Reines, and L. R. Price, "Modification by focused ultrasound pulses of electrically evoked responses from an in vitro hippocampal preparation," *Brain Res.*, vol. 558, no. 1, pp. 36–42, Aug. 1991.
- [11] W. J. Tyler, Y. Tufail, M. Finsterwald, and M. L. Tauchmann, "Remote excitation of neuronal circuits using low-intensity, low-frequency ultrasound," *PLoS One*, vol. 3, no. 10, p. e3511, 2008.
- [12] F. J. Fry, H. W. Ades, and W. J. Fry, "Production of reversible changes in the central nervous system by ultrasound," *Science*, vol. 127, no. 3289, pp. 83–84, Jan. 1958.
- [13] H. Kim, A. Chiu, S. D. Lee, K. Fischer, and S. S. Yoo, "Focused ultrasound-mediated non-invasive brain stimulation: Examination of sonication parameters," *Brain Stimulation*, vol. 7, no. 5, pp. 748–756, 2014.
- [14] R. L. King, J. R. Brown, W. T. Newsome, and K. B. Pauly, "Effective parameters for ultrasound-induced in vivo neurostimulation," *Ultrasound Med. Biol.*, vol. 39, no. 2, pp. 312–331, Feb. 2013.
- [15] Y. Tufail et al., "Transcranial pulsed ultrasound stimulates intact brain circuits," *Neuron*, vol. 66, no. 5, pp. 681–694, 2010.
- [16] S. Yoo et al., "Focused ultrasound modulates region-specific brain activity," *Neuroimage*, vol. 56, no. 3, pp. 1267–1275, 2011.
- [17] P.-H. Tsui, S.-H. Wang, and C.-C. Huang, "in vitro effects of ultrasound with different energies on the conduction properties of neural tissue," *Ultrasonics*, vol. 43, no. 7, pp. 560–565, Jun. 2005.
- [18] J. L. Foley, J. W. Little, and S. Vaezy, "Image-guided high-intensity focused ultrasound for conduction block of peripheral nerves," *Ann. Biomed. Eng.*, vol. 35, no. 1, pp. 109–119, Dec. 2006.
- [19] P. P. Ye, J. R. Brown, and K. B. Pauly, "Frequency dependence of ultrasound neurostimulation in the mouse brain," *Ultrasound Med. Biol.*, vol. 42, no. 7, pp. 1512–1530, Jul. 2016.
- [20] M. Plaksin, E. Kimmel, and S. Shoham, "Cell-type-selective effects of intramembrane cavitation as a unifying theoretical framework for ultrasonic neuromodulation," *eNeuro*, vol. 3, no. 3, Jun. 2016, Art. no. ENEURO.0136-15.2016.
- [21] J. Kubanek, P. Shukla, A. Das, S. A. Baccus, and M. B. Goodman, "Ultrasound elicits behavioral responses through mechanical effects on neurons and ion channels in a simple nervous system," *J. Neurosci.*, vol. 38, no. 12, pp. 3081–3091, Mar. 2018.
- [22] Y. Kung et al., "Focused shockwave induced blood-brain barrier opening and transfection," *Sci. Rep.*, vol. 8, no. 1, pp. 1–11, 2018.
- [23] H. Van Lier, W. H. Drinkenburg, Y. J. Van Eeten, and A. M. Coenen, "Effects of diazepam and Zolpidem on EEG beta frequencies are behavior-specific in rats," *Neuropharmacology*, vol. 47, no. 2, pp. 163–174, 2004.
- [24] H. W. Baac et al., "Carbon-nanotube optoacoustic lens for focused ultrasound generation and high-precision targeted therapy," *Sci. Rep.*, vol. 2, no. 1, pp. 1–8, 2012.
- [25] J. Kim et al., "Laser-generated-focused ultrasound transducers for microbubble-mediated, dual-excitation sonothrombolysis," in *Proc. IEEE Int. Ultrason. Symp. (IUS)*, Sep. 2016, pp. 1–4.
- [26] H. W. Baac, T. Lee, and L. J. Guo, "Micro-ultrasonic cleaving of cell clusters by laser-generated focused ultrasound and its mechanisms," *Biomed. Opt. Exp.*, vol. 4, no. 8, p. 1442, Aug. 2013.
- [27] J. Di, J. Kim, Q. Hu, X. Jiang, and Z. Gu, "Spatiotemporal drug delivery using laser-generated-focused ultrasound system," *J. Controlled Release*, vol. 220, pp. 592–599, Dec. 2015.
- [28] G. Kim, M. Kim, K. Ha, J. Lee, D.-G. Paeng, and M. J. Choi, "Waveform characteristics of ultrasonic wave generated from T/PDMS composite," *J. Acoust. Soc. Korea*, vol. 38, no. 4, pp. 459–566, 2019.
- [29] H. H. Jasper, "The ten-twenty electrode system of the international federation," *Electroencephalogr. Clin. Neurophys.*, vol. 10, pp. 370–375, Feb. 1958.
- [30] A. Shafique, M. Sayeed, and K. Tsakalis, "Nonlinear dynamical systems with chaos and big data: A case study of epileptic seizure prediction and control," in *Guide to Big Data Applications*. Cham, Switzerland: Springer, 2018, pp. 329–369.
- [31] J. Shen, B. Li, and X. Shi, "Real-time detection of human drowsiness via a portable brain-computer interface," *Open J. Appl. Sci.*, vol. 7, no. 3, pp. 98–113, 2017.
- [32] H. Suryotrisongko and F. Samopa, "Evaluating OpenBCI spiderclaw V1 headwear's electrodes placements for brain-computer interface (BCI) motor imagery application," *Proc. Comput. Sci.*, vol. 72, pp. 398–405, Jan. 2015.
- [33] S. Jiricek et al., "Electrical source imaging in freely moving rats: Evaluation of a 12-electrode cortical electroencephalography system," *Frontiers Neuroinform.*, vol. 14, Jan. 2021, Art. no. 589228.
- [34] (2017). *OpenBCI Github Repository [Internet]*. Accessed: April 24, 2021. [Online]. Available: <https://github.com/OpenBCI/ultracortex>
- [35] H. S. Sharma and P. K. Dey, "EEG changes following increased blood-brain barrier permeability under long-term immobilization stress in young rats," *Neurosci. Res.*, vol. 5, no. 3, pp. 224–239, Feb. 1988.
- [36] Z. Frehlick et al., "Human translingual neurostimulation alters resting brain activity in high-density EEG," *J. Neuroeng. Rehabilitation*, vol. 16, no. 1, pp. 1–7, 2019.
- [37] V. V. Vyazovskiy and I. Tobler, "Theta activity in the waking EEG is a marker of sleep propensity in the rat," *Brain Res.*, vol. 1050, nos. 1–2, pp. 64–71, Jul. 2005.
- [38] J. Lee, S. B. Zaigham, and D.-G. Paeng, "Shock wave characterization using different diameters of an optoacoustic carbon nanotube composite transducer," *Appl. Sci.*, vol. 12, no. 14, p. 7300, Jul. 2022.
- [39] K. Lin et al., "Histotripsy beyond the intrinsic cavitation threshold using very short ultrasound pulses: Microtriopsy," *IEEE Trans. Ultrason., Ferroelectr., Freq. Control*, vol. 61, no. 2, pp. 251–265, Feb. 2014.
- [40] T. Lee, W. Luo, Q. Li, H. Demirci, and L. J. Guo, "Laser-induced focused ultrasound for cavitation treatment: Toward high-precision invisible sonic scalpel," *Small*, vol. 13, no. 38, Oct. 2017, Art. no. 1701555.
- [41] T. D. Khokhlova, Y. A. Haider, A. D. Maxwell, W. Kreider, M. R. Bailey, and V. A. Khokhlova, "Dependence of boiling histotripsy treatment efficiency on HIFU frequency and focal pressure levels," *Ultrasound Med. Biol.*, vol. 43, no. 9, pp. 1975–1985, Sep. 2017.
- [42] Z. Xu, T. L. Hall, E. Vlaisavljevich, and F. T. Lee, "Histotripsy: The first noninvasive, non-ionizing, non-thermal ablation technique based on ultrasound," *Int. J. Hyperthermia*, vol. 38, no. 1, pp. 561–575, Jan. 2021.
- [43] T. Sato, M. G. Shapiro, and D. Y. Tsao, "Ultrasonic neuromodulation causes widespread cortical activation via an indirect auditory mechanism," *Neuron*, vol. 98, no. 5, pp. 1031–1041, Jun. 2018.
- [44] J. Blackmore, S. Shrivastava, J. Sallet, C. R. Butler, and R. O. Cleveland, "Ultrasound neuromodulation: A review of results, mechanisms and safety," *Ultrasound Med. Biol.*, vol. 45, no. 7, pp. 1509–1536, 2019.